How to cite: *Angew. Chem. Int. Ed.* **2025**, *64*, e202419531
doi.org/10.1002/anie.202419531

VIP Dynamic Covalent Exchange Very Important Paper

Dynamic Covalent Spiropyran Exchange for Rapid Structural Diversification

Alwin Drichel, Yves Garmshausen, and Stefan Hecht**

Abstract: Here we disclose that spiropyrans are able to undergo dynamic covalent exchange via their corresponding merocyanine isomers. In the latter, the indolinium moieties can be exchanged by a Michael-type addition-elimination sequence, in which a methylene indoline attacks a merocyanine and subsequently the initial indoline fragment is cleaved. The rate and position of the exchange equilibrium strongly depend on the reaction conditions as well as the substitution pattern on the methylene indoline fragments. Importantly, spiropyran cross exchange is catalyzed by indolinium salts and provides the opportunity for rapid in situ structural diversification of spiropyrans. This was used as synthetic tool to access various, hitherto inaccessible spiropyrans as potential dual-color photoinitiators for xolography. Moreover, we foresee application to screen dynamic covalent libraries of spiropyrans for photochromic properties and to exploit their light-sensitivity to bias the thermal equilibrium.

[*] A. Drichel
DWI-Leibniz Institute for Interactive Materials
Forckenbeckstr. 50, 52074 Aachen, Germany
and
Institute of Technical and Macromolecular Chemistry
RWTH Aachen University, Worringerweg 1, 52074 Aachen, Germany

Dr. Y. Garmshausen
xolo GmbH
Volmerstraße 9B, 12489 Berlin, Germany
E-mail: yves.garmshausen@xolo3d.com

Prof. Dr. S. Hecht
Department of Chemistry, Humboldt-Universität zu Berlin
Brook-Taylor-Str. 2, 12489 Berlin, Germany
and
Center for the Science of Materials Berlin
Humboldt-Universität zu Berlin
Zum Großen Windkanal 2, 12489 Berlin, Germany
and
DWI-Leibniz Institute for Interactive Materials
Forckenbeckstr. 50, 52074 Aachen, Germany
and
Institute of Technical and Macromolecular Chemistry
RWTH Aachen University, Worringerweg 1, 52074 Aachen, Germany
E-mail: sh@chemie.hu-berlin.de

Introduction

During the discovery of spiropyrans by Decker in 1908, the marked reactivity difference between the open and closed isomer has already been shown. In Decker's case, the nucleophilic addition of hydroxide to the open merocyanine resulted in formation of the light yellow carbinol oxonium salt (Figure 1), while the closed spiropyran remained unaffected.[1] In general, the spiropyran isomer can undergo a reversible ring-opening, in which the C–O bond at the spiro center breaks, resulting in the formation of the merocyanine isomer. The latter typically is thermodynamically less stable and isomerizes back to the spiropyran via thermal ring-closure. As a result of the isomerization process, the isomers' physicochemical properties such as ground state and transition dipole moments as well as light absorbance drastically change.[2–4] Over the past decades, multiple stimuli to induce this isomerization process were uncovered such as pH,[1,5] temperature,[6] light,[7] and mechanical force.[8] Due to these vast possibilities to switch between the spiropyran and merocyanine isomers and the resulting large modulation of their physicochemical properties, spiropyrans have been prominently employed in various applications ranging from ion-, chemo-, and stress-sensing[9–15] over pH-modulation[16–18] all the way to dual-color photoinitiation in xolography.[19]

As already indicated in the original work by Decker,[1] a key difference between the two isomers is their reactivity with nucleophiles. While the spiropyran isomer is not affected by them, nucleophilic addition to the merocyanine isomer can commonly occur by 1,2- or 1,4-attack on the α,β-unsaturated iminium ion.[20] Over time, multiple nucleophilic reactions were discovered (Figure 1). In the beginning, 1,2-additions with hard nucleophiles such as hydroxide[1,21] and cyanide[13,20] were uncovered, followed by conjugate 1,4-additions of softer nucleophiles such as thiols[22] and sulfite.[14,15] The reaction of primary and secondary amines with merocyanines resulted in the formation of imines and methylene indolines. To account for this observation, Tian and co-workers suggested a 1,4-addition of the amine to the merocyanine followed by the elimination of methylene indoline.[23]

Here we report on the dynamic covalent nature of the C=C double bond present in the merocyanine isomer (Figure 1). While the C=C double bond is locked and stable towards nucleophilic attack in the closed spiropyran isomer, it can be unlocked by thermal interconversion to the merocyanine isomer. Subsequent nucleophilic addition of an external indoline moiety to the merocyanine and the

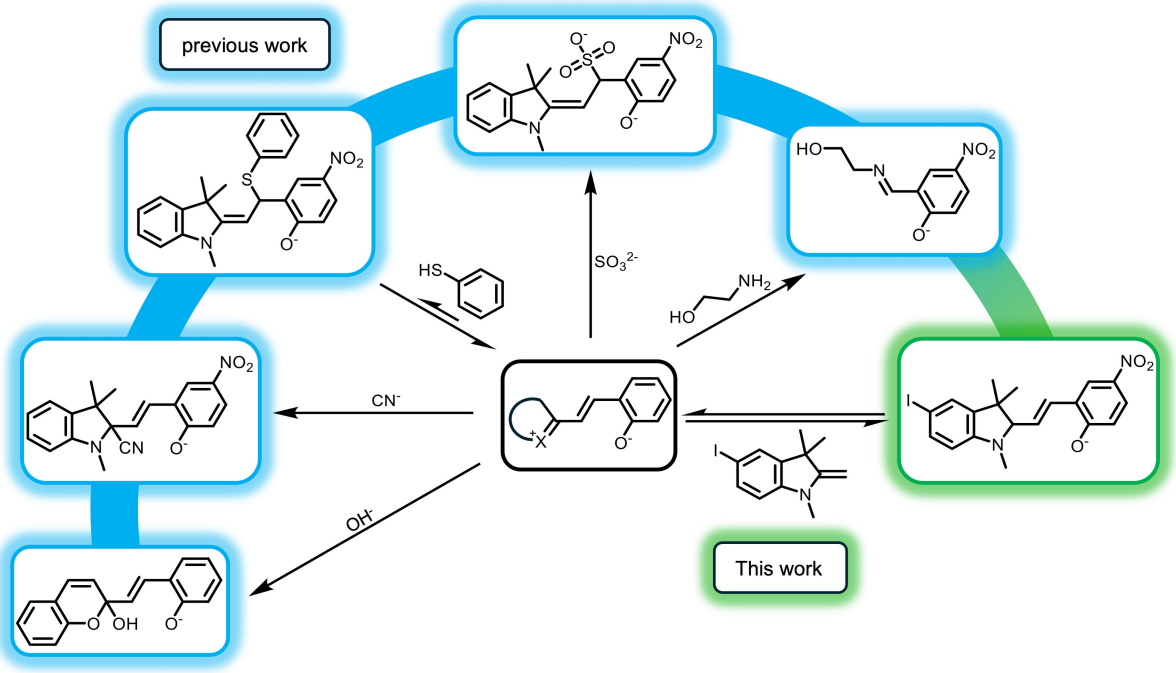

Figure 1. Evolution of nucleophilic additions to merocyanines formed via solvatochromism or photochromism. Blue: Previous work consisting of 1,2-addition of hydroxide[1] and cyanide,[13] followed by 1,4-addition of thiols,[22] sulfite,[15] and amines.[23] Green: Scope of this work demonstrating dynamic covalent spiropyran exchange via reversible 1,4-addition/elimination.

subsequent release of the initially present indoline moiety results in the formation of a new merocyanine. Thermal ring-closure locks the double bond again and leads to a new spiropyran with an exchanged indoline moiety. The equilibrium in such exchanging spiropyran systems critically depends on the thermal stability of the merocyanine as well as the electronic nature of both indoline moieties.

Dynamic covalent chemistry (DCC) is uniquely suited for rapid in situ structural diversification. Previously, we have exploited DCC based on reversible Knoevenagel condensation to create and efficiently screen a dynamic constitutional library of α-cyanodiarylethene photoswitches.[24] In the context of generating a wide variety of spiropyrans, for example as potential dual-color photoinitiators, dynamic covalent exchange provides a powerful synthetic tool. Moreover, available synthetic methods to diversify spiropyrans and their substitution patterns suffer from their chemical sensitivity towards many post-functionalization conditions. Alternative routes involving the synthesis of various salicylaldehyde precursors are limited due to the electronic nature of the substrates. Functionalization is limited due to the electronic nature of the salicylaldehydes and their sensitivity to nucleophiles, oxidative and reductive conditions. Therefore, reactions on salicylaldehydes often require two protection and deprotection steps for the hydroxy group and the aldehyde, respectively.[25–27] Interestingly, indolines have been used as a protecting group for salicylaldehydes that after successful transformation was cleaved by ozonolysis.[28] Due to the strong directing effect of the hydroxyl group, functionalization is limited to the *para* position to the hydroxyl group and the strong electron withdrawing aldehyde results in a deactivation of the aromatic system. Therefore, only very reactive electrophiles such as acetic anhydride with aluminum chloride are able to undergo a direct functionalization of salicylaldehyde. Other methods to obtain salicylaldehydes such as *ortho*-formylation of phenols are limited as well and require electron-rich aromatic systems to obtain the desired product in acceptable yields.[29–31] By using the spiropyran exchange, however, we are able to synthesize potential dual-color photoinitiators for xolography, which would otherwise be unobtainable.

Results and Discussion

Initially, we discovered an exchange between two distinct spiropyrans by in situ ^{1}H NMR (Figure 2). Both spiropyrans **SP1** and **SP2** were dissolved in ethanol-d6 in equimolar amounts (15 mM) together with 0.2 equiv. of water and heated for multiple days at 70 °C. After 3 days, new signals appear with chemical shifts of $\delta = 2.68$ and 2.73 ppm, which correspond to the N-CH_3 groups of **SP3** and **SP4**. The formation of both of these spiropyrans can be observed in the aromatic region at 6.30 and 6.52 ppm diagnostic for the indoline protons as well. Moreover, the formation of some salicylaldehyde is observed as indicated by the signal at 10.0 ppm.

For the spiropyran cross exchange to occur, two plausible pathways (Figure 3) have been considered, which both rely on thermal equilibration between the spiropyrans and their more reactive merocyanine forms. Perhaps the more obvious pathway involves thermal ring-opening of the initial

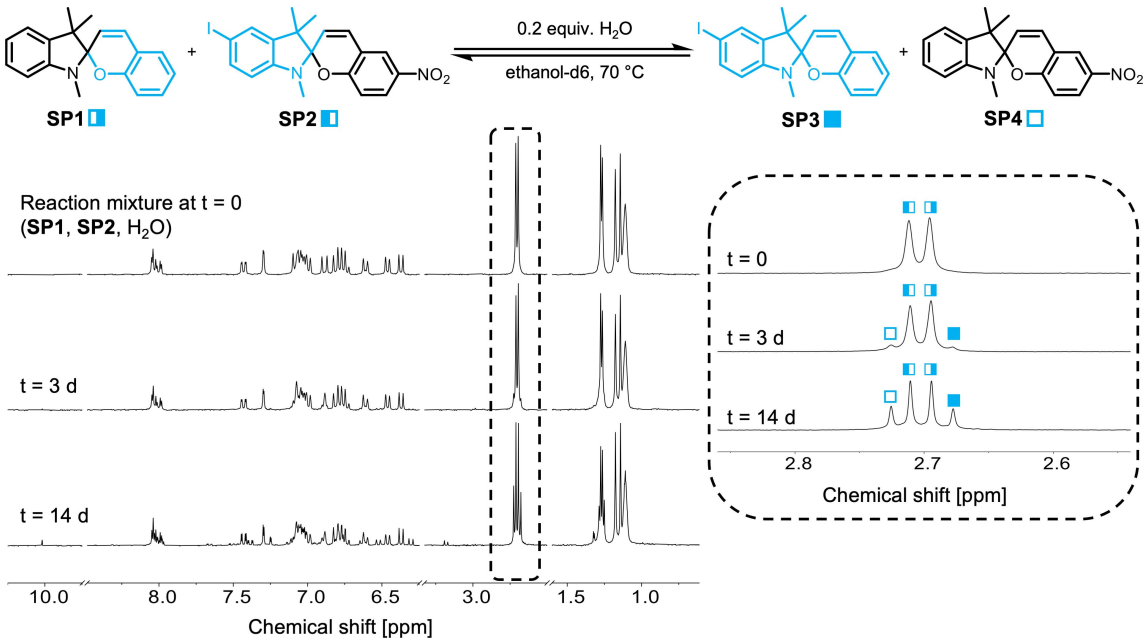

Figure 2. Water-catalyzed spiropyran cross exchange between **SP1** and **SP2**. a) In situ ^{1}H NMR monitoring ([**SP1**]=[**SP2**]=15 mM, [H_2O]=3 mM in C_2D_5OD, 70 °C, 300 MHz) and b) zoomed section between 2.86 and 2.54 ppm.

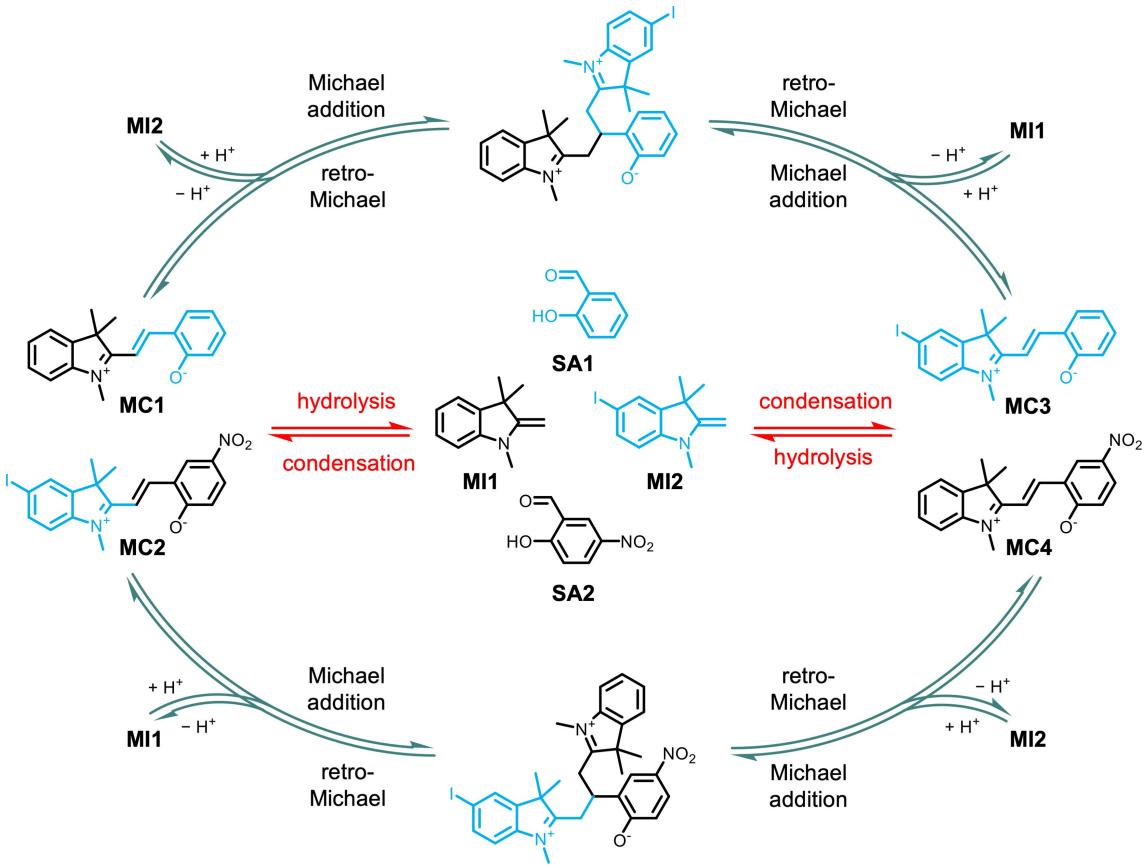

Figure 3. Mechanistic scenarios to account for spiropyran cross exchange via their corresponding merocyanines. Two plausible pathways involve either i) complete hydrolysis of both merocyanines **MC1** and **MC2** to yield salicylaldehydes **SA1** and **SA2** as well as methylene indolines **MI1** and **MI2** followed by their re-condensation to form the new combinations **MC3** and **MC4** (middle, red arrows) or ii) partial hydrolysis to generate **MI1** and **MI2**, which can induce exchange via nucleophilic 1,4-addition to **MC1** and **MC2**, respectively, followed by elimination of the opposite methylene indoline fragments to form merocyanines **MC3** and **MC4** (top and bottom, green arrows).

SP1 and **SP2** to form the corresponding **MC1** and **MC2**, followed by hydrolysis of both merocyanines. The formed pairs of methylene indolines and salicylaldehydes are able to re-condense without restriction, resulting in the formation of the four possible merocyanines **MC1**-**MC4**. Thermal ring-closure of **MC3** and **MC4** would give their corresponding spiropyrans **SP3** and **SP4**. The alternative pathway requires only partial hydrolysis of **MC1**, leading to formation of methylene indoline **MI1** and salicylaldehyde **SA1**. **MI1** is a nucleophile, which can react in a Michael-type 1,4-addition with **MC2** and result in the formation of an adduct, which contains both indoline moieties. Elimination of **MI2** results in the formation of **MC4**, which subsequently closes thermally to **SP4**. The released **MI2** either condenses with **SA1** to form **MC3**, stopping the exchange process and requiring hydrolysis to generate a new nucleophile for further exchange to occur or alternatively attacks **MC1** to give **MI1** and **MC3** while keeping an active nucleophile in the system. A similar exchange mechanism has been shown by Di Stefano and co-workers to operate in the case of amine-catalyzed imine metathesis.[32]

We were intrigued by the possibility of the latter mechanism that does not rely on (trivial) full hydrolysis and should potentially result in a faster exchange. In addition, we were interested to investigate the effect of different substitution patterns on the indoline as well as spiropyran/merocyanine moieties on the exchange distribution. Therefore, an exemplary exchange between **SP4** and **MI2** as well as the reverse reaction between **SP2** and **MI1** were carried out (Figure 4). Note that **MI1** and **MI2** were generated in situ through deprotonation of their corresponding indolinium salts.

In situ ^{1}H NMR monitoring of the spiropyran exchange (Figure 4a) shows that formation of the exchange products **SP2** and **MI1** is already observable after 10 min by the onset of the distinct proton signals of the N-CH_3 groups in **SP2** at 2.71 ppm and **MI1** at 3.01 ppm. Besides the equilibrating spiropyrane (**SP4**, **SP2**) and methylene indoline (**MI1**, **MI2**) species as well as the piperidinium ions (multiplet of N-CH_2 protons at 2.85 ppm), no other species could be detected by ^{1}H NMR (**Figure S1**). In comparison to the cross exchange, the rate of exchange dramatically increased and equilibrium was reached after 360 min leading to an almost equal distribution of **SP2**:**SP4** = 49:51 (Figure 4b, blue symbols). Full equilibration was proven by approaching equilibrium from the reverse direction, i.e. starting from **SP2** and **MI1** and resulting in the same distribution (Figure 4b, red symbols). Based on these observations as well as considering reports of 1,4-addition in the literature,[14,22,23] we conclude that the addition and elimination pathway is more likely to occur than the hydrolysis and condensation pathway. While in the above spiropyran exchange (Figure 4) an over-stoichiometric amount of piperidine was used to ensure complete activation of the methylene indolines in the system, we subsequently found that a base for the deprotonation of the indolinium salt is not required. Instead, the thermally formed merocyanine acts as a base, leading to its stabilization by protonation of the phenoxide and simulta-

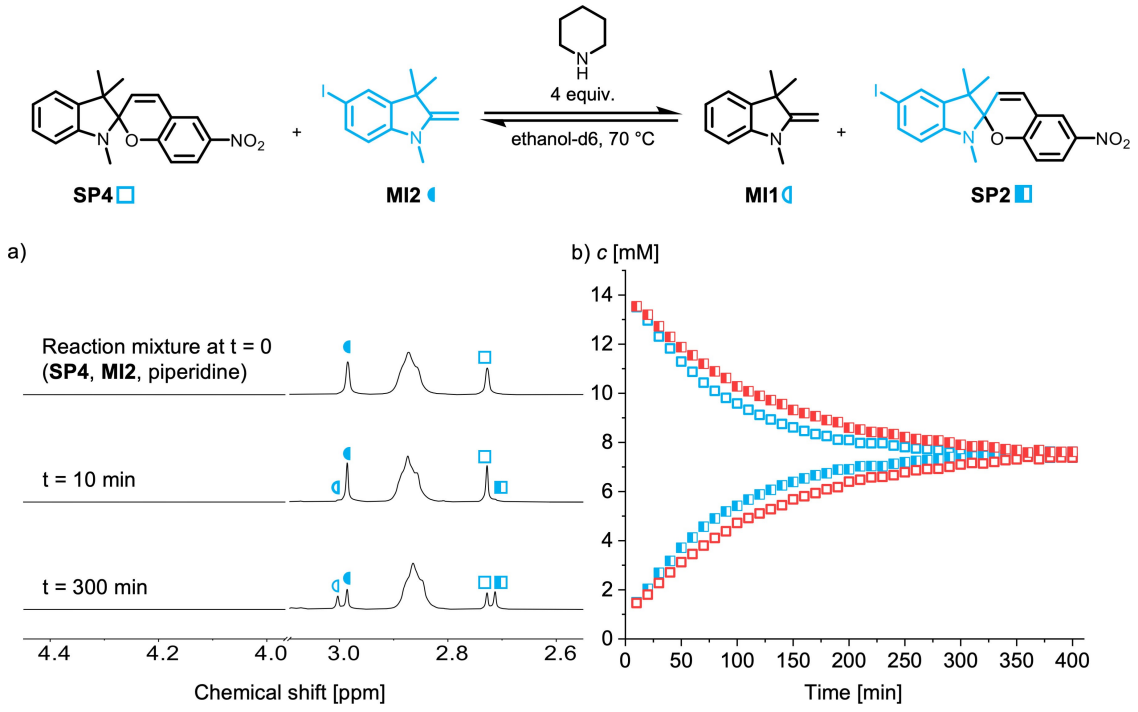

Figure 4. Spiropyran exchange between **SP4** + **MI2** and **SP2** + **MI1** in presence of excess base: a) in situ ^{1}H NMR monitoring ([**SP4**] = [**MI2**] = 15 mM, [piperidine] = 60 mM, in C_2D_5OD, 70 °C, 300 MHz) and b) resulting spiropyran concentration evolution as determined by integrating N-CH_3 signals at 2.73 ppm (**SP4**) and 2.71 ppm (**SP2**). Blue symbols correspond to the forward process starting from **SP4** and **MI2**, while the back reaction starting from **SP2** and **MI1** is represented by red symbols.

neous activation of the methylene indoline for the exchange. The applicability of such base-free exchange conditions was demonstrated by the exemplary exchange of spiropyran **SP4** using the indolinium salt **In1** as well as the reverse reaction (Figure 5). Already in the initial ^{1}H NMR spectrum, formation of **MCH4** and **MI2** through deprotonation of **In1** by **MC1** can be observed (Figure 5a). In comparison to the initial spiropyran exchange using excess base (Figure 4), equilibrium is reached significantly faster, i.e. within 210 min instead of 360 min. Without the addition of base, the equilibrium distribution of **SP2:SP4** shifts from 49:51 to 74:26 clearly favoring formation of **SP2**.

There are multiple plausible explanations for the increased equilibration rate and the change in the equilibrium distribution. First, protonation greatly enhances the stability of the merocyanine, resulting in a higher concentration of the open reactive iminium ion and therefore in an increase of the exchange rate. Note that the non-protonated merocyanines could not be observed in either exchange conditions, only the protonated ones are visible in the ^{1}H NMR spectrum (Figures 4a, 5b). Second, the concentration of **MCH4** is higher than **MCH2** in equilibrium (Figure 5b), which may be explained by better stabilization of the cation by hydrogen as the *para*-substituent on the indoline part as compared to the electron-withdrawing iodo-substituent.[33] Since the reactive species in the exchange reaction is the merocyanine, the resulting distribution of the spiropyrans is dictated by the ratio of the protonated merocyanines and their (de)stabilizing substituents, respectively. Moreover, the exchange distribution depends on the substitution patterns of the methylene indolines as well. As the protonated indolinium salts and the deprotonated methylene indolines are in equilibrium, favored deprotonation of the more acidic **In2** by **MI1** leads to an increased concentration of **MI2** (and **In1**), which leads to preferential formation of the resulting **SP2** (Figure 5a).

Similar results were also obtained in the case of spiropyrans **SP1** and **SP3**, which do not carry a nitro group, in combination with the respective indolines (see **Figures S5** and **S6**). The absence of a nitro group in the exchange systems causes the reactivity to decrease since equilibrium is reached only after 460 min. Although the exchange systems with **SP1** and **SP3** favor formation of the protonated merocyanines when compared to the exchange systems with **SP2** and **SP4** (see **Figures S3b-S6b**), the strong electron-withdrawing nature of the nitro-group appears to substan-

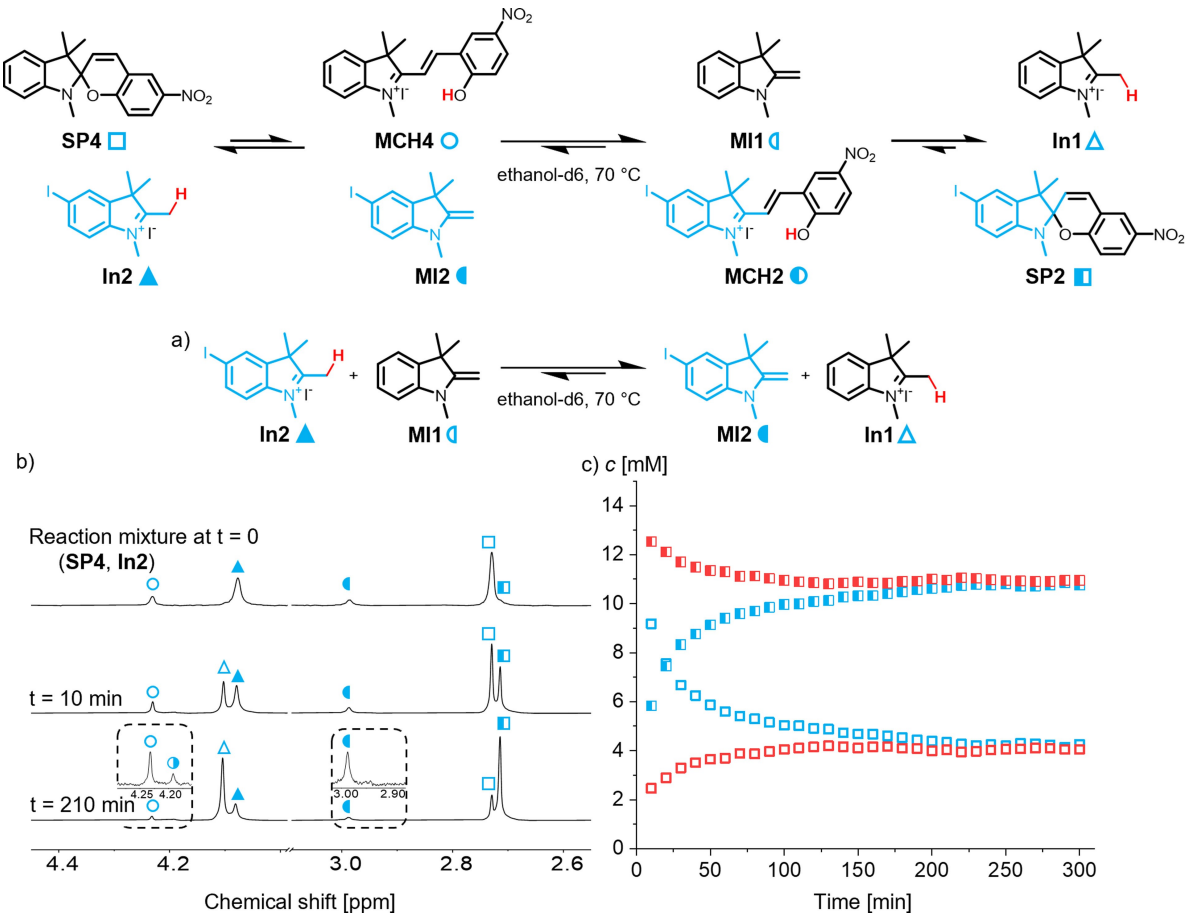

Figure 5. Base-free spiropyran exchange between **SP4** + **In2** and **SP2** + **In1**: a) additional protonation equilibrium between both methylene indolines and indolinium salts, b) in situ ^{1}H NMR monitoring ([**SP4**] = [**In2**] = 15 mM, in C_2D_5OD, 70 °C, 300 MHz), c) resulting spiropyran concentration evolution as determined by integrating N-CH_3 signals at 2.73 ppm (**SP4**) and 2.71 ppm (**SP2**). Blue symbols correspond to the forward process starting from **SP4** and **In2**, while the back reaction starting from **SP2** and **In1** is represented by red symbols.

tially increase the electrophilicity of the merocyanines, resulting in an overall faster exchange rate even though the concentration of the active exchange species is lower.

To elucidate the effect of methylene indoline substitution on spiropyran exchange, various *para*-functionalized indolinium salts (**In3-6**) were investigated in combination with **SP4** (Figure 6).

From the analysis of the individual exchange reactions (see **Figures S3**, **S7**, **S9**, and **S11**) it is apparent that by increasing the electron-withdrawing nature of the *para*-substituent of the indolinium salt, the equilibrium shifts towards formation of the exchanged spiropyrans. Thus, the equilibrium clearly favors the acceptor-substituted spiropyran with almost complete conversion in case of **SP4** (*p*-H)→ **SP6** (*p*-CO_2Et) and **SP4** (*p*-H)→**SP7** (*p*-CF_3). The logarithmic plot of the equilibrium constants (log (K_{ex})) against the Hammett constants (σ_p) shows a linear correlation (Figure 6b). Equilibration was verified by carrying out the exchange in the opposite direction, i.e. reacting **SP5-7** with **In1** (see **Figures S8**, **S10**, and **S12**).

Comparing the rates and extent of equilibration for the various exchange scenarios of starting from the less/more favored spiropyran and reacting with a more/less acidic indolinium salt shows the influence of various factors. These include the inherent electrophilicity and nucleophilicity of the intermediate merocyanines and methylene indolines, respectively, as well as their concentration, which depend on the acid-base equilibrium between indolinium salt and merocyanine as well as the thermal stability of the latter. This is illustrated by the fact that strong electron-withdrawing substituents in *para*-position destabilize the merocyanine resulting in a lower probability to deprotonate the indolinium salt and thus induce exchange. Thus, in the **SP4** ↔ **SP6** and **SP4** ↔ **SP7** exchange systems the corresponding merocyanines **MCH6** and **MCH7**, respectively, could not be observed (see **Figures S9–S12**). Importantly, the acid-base equilibrium between indolinium salts and methylene indolines favors formation of the methylene indoline with the stronger electron-withdrawing group as the active species, while the methylene indoline with the weaker electron-withdrawing group is protonated and therefore unable to participate in the exchange. As a consequence, the spiropyran carrying the stronger electron-withdrawing group will be formed preferentially.

Taking advantage of the gained mechanistic understanding, the initial spiropyran cross exchange was optimized. Instead of using water as a hydrolysis catalyst, **In1** was used, which resulted in a drastic increase in the exchange rate between spiropyrans **SP1** and **SP2** to form spiropyrans **SP3** and **SP4** (Figure 7). While in the aqueous catalyst system 3 days were needed to observe exchange, the same amount of exchange products could be observed after 1 h using the indolinium salt (see **Figure S13**). The reactivity boost is due to the acid-induced ring opening that generates both reactants, i.e. the protonated merocyanine electrophile and the methylene indoline nucleophile.

As a first demonstration of the applicability of spiropyran exchange we utilized it for the synthesis of dual-color photoinitiators, which can be used in xolography.[19] In this volumetric 3D printing method, local polymerization within a resin vat is induced by intersecting light beams of different wavelengths. To achieve fast printing speed while maintaining high resolution, the thermal half-life of the merocyanine needs to be fine-tuned and ideally be rather short.[19] The

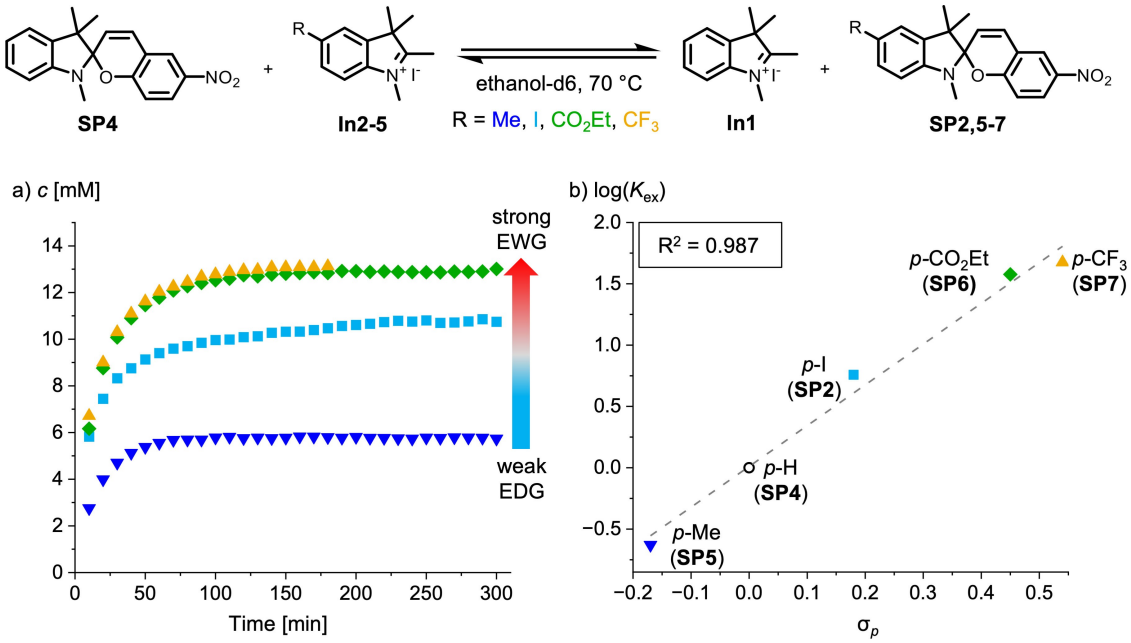

Figure 6. Spiropyran exchange between **SP4** and various *para*-substituted indolinium salts (**In2-5**): a) Combined spiropyran and merocyanine concentration evolution as determined by integrating N-CH_3 signals (see **Figures S3**, **S7**, **S9**, and **S11**). b) Hammett plot of the equilibrium distribution, i.e. log(K_{ex}) against σ_p.

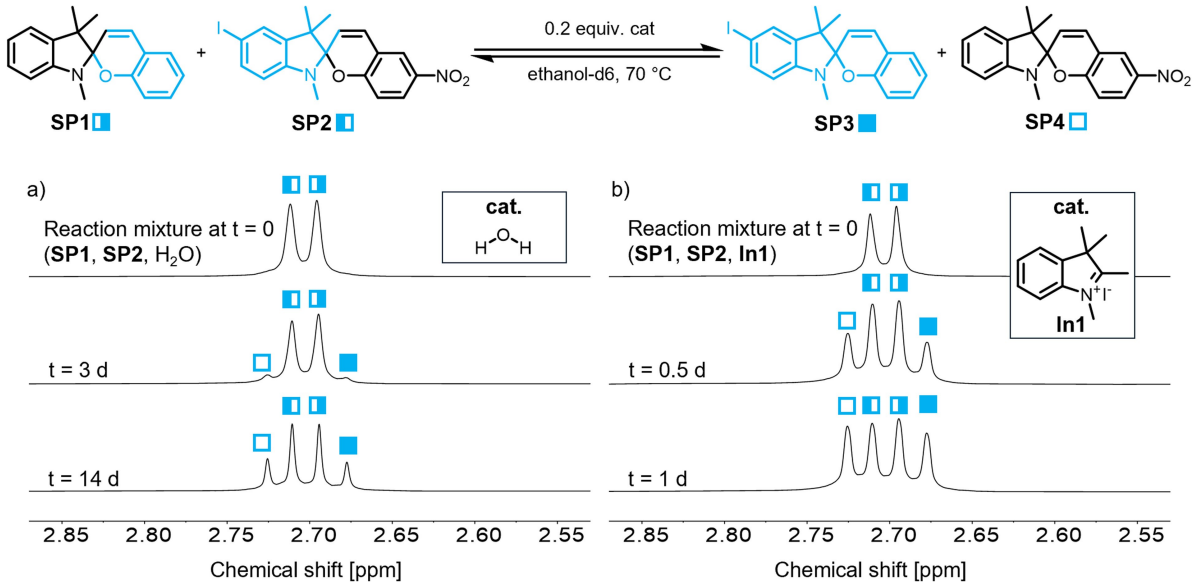

Figure 7. Spiropyran cross exchange between **SP1** and **SP2** as monitored by in situ ^{1}H NMR : a) Water-catalyzed spiropyran cross exchange, b) indolinium salt-catalyzed spiropyran cross exchange ([**SP1**] = [**SP2**] = 15 mM, [catalyst] = 3 mM in C_2D_5OD, 70 °C, 300 MHz).

latter can be realized by introducing electron-poor indoline moieties,[33] which however are synthetically difficult to introduce. To circumvent these problems, we took advantage of the spiropyran exchange as mild late-stage diversification tool by using the unsubstituted parent indoline moiety as a protecting group during functionalization of the chromene moiety (Figure 8).

Halogen-metal-exchange of a halogenated spiropyran with *n*-butyl lithium and further reaction with a Weinreb amide enables acylation in any position of the spiropyran, especially the chromene, while a Friedel–Crafts acylation typically targets the 6'-position. Exemplarily, acylation in the otherwise not accessible 5'-position as well as acylation in 6'-position of an electron-poor chromene moiety were performed. The synthesis of **SP10-12** as well as **SP15** and

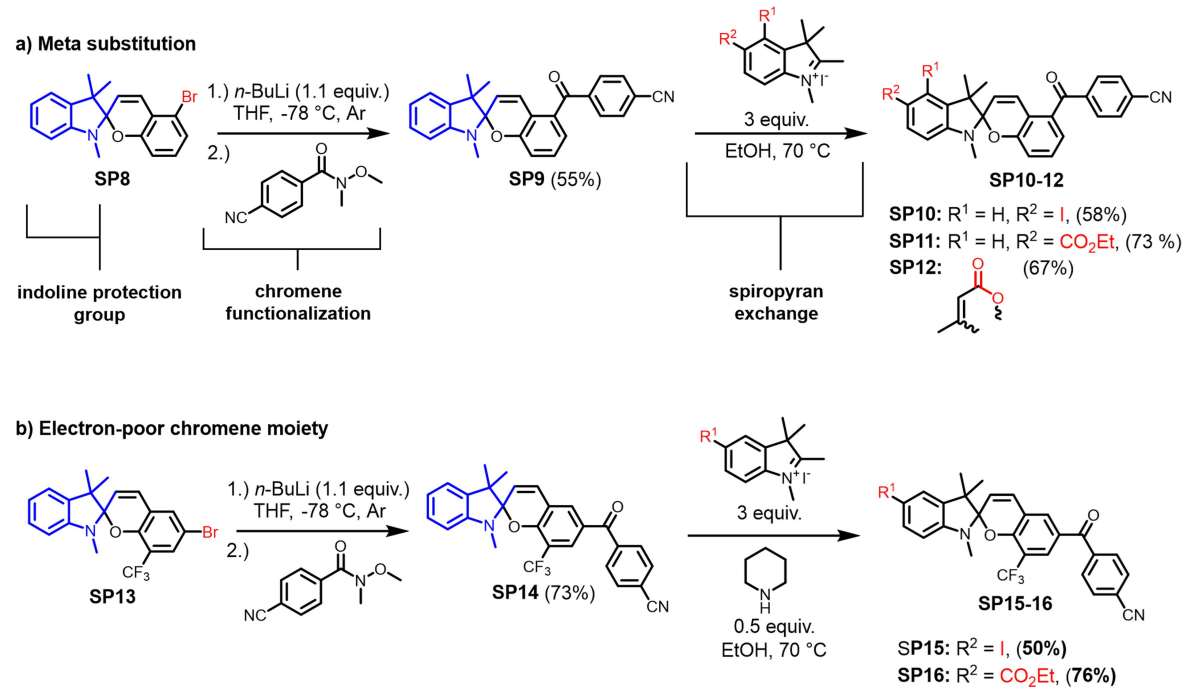

Figure 8. Synthesis of potential dual-color photoinitiators based on spiropyran exchange as late-stage diversification to access: a) 5'-benzoyl and b) 6'-benzoyl (8'-CF_3) substituted spiropyrans **SP10-12** and **SP15**,**16**.

SP16 through modification such as Friedel–Crafts acylation of salicylaldehydes or *ortho*-formylation of phenols are not possible.[2–31] The substituents introduced during the exchange reaction are not compatible with halogen-metal-exchange, i.e. *n*-butyl lithium. To obtain higher yields of the exchange product, 3 equivalents of the indolinium salts were used. Due to the electron-poor chromene moiety in **SP14**, a sub-stoichiometric amount of piperidine was added. In this case, the electron-withdrawing groups render the phenoxide moiety of **MC14** not basic enough to deprotonate the indolinium salt sufficiently. Therefore, an additional base, i.e. piperidine, was added to activate the nucleophile for the exchange. Gratifyingly, the spiropyran exchange proved to be an effective method for the synthesis of various spiropyran derivatives, unattainable by other routes, in yields ranging up to 76 %.

Conclusion

In the course of this work, we discovered the ability of spiropyrans to undergo dynamic covalent exchange reactions via their latent merocyanine isomers. We systematically investigated substrate scope by varying their substitution pattern and optimized reaction conditions. Key to enable efficient spiropyran exchange is the use of indolinium salts. The latter engage in facile proton-transfer to merocyanines (thermally generated from spiropyrans) leading to formation of methylene indoline (enamine) nucleophiles and long-lived protonated merocyanine electrophiles. These undergo a Michael addition-elimination sequence that swaps the indoline fragments. The position of the resulting equilibrium depends on the electronic nature of the same *para*-substituents that control the methyl indolines' nucleophilicity as well as the (protonated) merocyanines' electrophilicity as shown by a Hammett analysis. The equilibration time is moreover affected by the concentration of these key reactive intermediates, which relate to the underlaying acid-base equilibria and the thermal half-life of the merocyanines.

An optimized exchange protocol was used to synthesize spiropyrans, which cannot be synthesized through other routes, demonstrating an efficient way to access a wide variety of potential dual-color photoinitiators. In addition, we are currently exploring our exchange conditions to screen dynamic covalent spiropyran libraries for specific photochromic properties, complementing and expanding our previous work in the context of diarylethenes.[24] Moreover, we are investigating the influence of irradiation in order to bias and drive dynamic covalent exchange equilibria[34–37] for potential use in photoresponsive material systems.[38, 39]

Supporting Information

Additional Data, which supports the findings of his study, is available in the supplementary material of this article.

Acknowledgements

We thank Ines Bachmann-Remy for help with the in situ ^{1}H NMR measurements as well as Jutta Schwarz, Jannes Leonhard, and Linos Madalo for synthesis support. Funding by the Deutsche Forschungsgemeinschaft (DFG via SPP 2363 "Molecular Machine Learning") is gratefully acknowledged. S.H. thanks the Einstein Foundation Berlin as well as Humboldt University for generous support. Open Access funding enabled and organized by Projekt DEAL.

Conflict of Interest

Stefan Hecht is co-founder of xolo GmbH.

Data Availability Statement

The data that support the findings of this study are available in the supplementary material of this article.

Keywords: Dynamic Covalent Chemistry · Merocyanine · Spiropyran · Xolography

[1] H. Decker, H. Felser, *Ber. Dtsch. Chem. Ges.* **1908**, *41*, 2997–3007.
[2] Q. Shen, Y. Cao, S. Liu, M. L. Steigerwald, X. Guo, *J. Phys. Chem. C* **2009**, *113*, 10807–10812. 10.1021/jp9026817.
[3] M. Levitus, G. Glasser, D. Neher, P. F. Aramendia, *Chem. Phys. Lett.* **1997**, *277*, 118–124. 10.1016/S0009-2614(97)00826-9.
[4] M. Bletz, U. Pfeifer-Fukumura, U. Kolb, W. Baumann, *J. Phys. Chem. A* **2002**, *106*, 2232–2236. https://doi.org/10.1021/jp012562q.
[5] S. Keum, K. Lee, P. M. Kazmaier, E. Buncel, *Tetrahedron Letters* **1994**, *35*, *7*, 1015–1018. 10.1016/S0040-4039&DELETE;TRzwj;(00)79953-9.
[6] A. Löwenbein, W. Katz, *Ber. Dtsch. Chem. Ges.* **1926**, *59*, 1377–1383. 10.1002/cber.19260590704.
[7] E. Fischer, Y. Hirshberg, *J. Chem. Soc.* **1952**, 4522–4524.
[8] D. S. Tipikin, *Russ. J. Phys. Chem.* **2001**, *75*, 1720–1722.
[9] S. L. Potisek, D. A. Davis, N. R. Sottos, S. R. White, J. S. Moore, *J. Am. Chem. Soc.* **2007**, *129*, 13808–13809. 10.1021/ja076189x.
[10] D. A. Davis, A. Hamilton, J. Yang, L. D. Cremar, D. Van Gough, S. L. Potisek, M. T. Ong, P. V. Braun, T. J. Martinez, S. R. White, J. S. Moore, N. R. Sottos, *Nature* **2009**, *459*, 68–72. 10.1038/nature07970.
[11] J. P. Phillips, A. Mueller, F. Przystal, *J. Am. Chem. Soc.* **1965**, *87*, 4020.
[12] N. Shao, Y. Zhang, S. Cheung, R. Yang, W. Chan, T. Mo, K. Li, F. Liu, *Anal. Chem.* **2005**, *77*, 7294–7303. 10.1021/ac051010r.
[13] Y. Shiraishi, K. Adachi, M. Itoh, T. Hirai, *Org. Lett.* **2009**, *11*, *15*, 3482–3485. 10.1021/ol901399a.
[14] J. Zhang, Y. Fu, H. Han, Y. Zang, J. Li, X. He, B. L. Feringa, H. Tian, *Nat. Commun.* **2017**, *8*, 987. 10.1038/s41467-017-01137-8.
[15] X. Li, Z. Lin, Y. Tian, C. Zhang, P. Zhang, R. Zeng, L. Qiao, J. Chen, *Anal. Bioanal. Chem.* **2023**, *415*, 715–724. 10.1007/s00216-022-04462-0.
[16] Z. Shi, P. Peng, D. Strohecker, Y. Liao, *J. Am Chem. Soc.* **2011**, *133*, 14699–14703.https://doi.org/10.1021/ja203851c.

[17] L. Wimberger, S. K. K. Prasad, M. D. Peeks, J. Andréasson, T. W. Schmidt, J. E. Beves, *J. Am. Chem. Soc.* **2021**, *143*, 20758–20768. 10.1021/jacs.1c08810.
[18] G. Vozzolo, F. Elizalde, D. Mantione, R. Aguirresarobe, M. Ximenis, H. Sardon, *Polymer* **2024**, *302*, 127051. 10.1016/j.polymer.2024.127051.
[19] M. Regehly, Y. Garmshausen, M. Reuter, N. F. König, E. Israel, D. P. Kelly, C. Chou, K. Koch, B. Asfari, S. Hecht, *Nature* **2020**, *588*, 620–624. 10.1038/s41586-020-3029-7.
[20] A. Perry, *Org. Biomol. Chem.* **2019**, *17*, 4825. 10.1039/C9OB00641A.
[21] C. Liu, Y. Lu, S. He, Q. Wang, L. Zhao, X. Zeng, *J. Mater. Chem. C* **2013**, *1*, 4770. 10.1039/C3TC30768A.
[22] Y. Shiraishi, K. Yamamoto, S. Sumiya, T. Hirai, *Phys. Chem. Chem. Phys.* **2014**, *16*, 12137. 10.1039/C3CP55478C.
[23] Y. Xue, J. Tian, W. Tian, K. Zhang, J. Xuan, X. Zhang, *Spectrochimica Acta Part A: Molecular and Biomolecular Spectroscopy* **2021**, *250*, 119385. 10.1016/j.saa.2020.119385.
[24] N. König, D. Mutruc, S. Hecht *J. Am. Chem. Soc.* **2021**, *143*, 9162–9168. 10.1021/jacs.1c03631.
[25] M. Zaidlewicz, A. Wolan, *Journal of Organometallic Chemistry* **2002**, *657*, 129–135.
[26] S J. Gharpure, A. M. Sathiyanarayanana, P. K. Vurama, *RSC Advances* **2013**, *3*, 18279. 10.1039/C3RA43526A.
[27] X. Zhu, K. N. Plunkett. *J. Org. Chem.* **2014**, *79*, 7093–7102. 10.1021/jo501266g.
[28] Y. J. Cho, S. H. Lee, J. W. Bae, H. Pyun, C. M. Yoon, *Tetrahedron Letters* **2000**, *41*, 3915–3917. 10.1016/S0040-4039(00)00516-5.
[29] J. C. Duff, *J. Chem. Soc.* **1941**, 547–550. 10.1039/JR9410000547.
[30] N. U. Hofsløkken, L. Skattebøl, *Acta Chem. Scand.* **1999**, *53*, 258.
[31] H. Wynberg, *Chem. Rev.* **1960**, *60*, *2*, 169–184. 10.1021/cr60204a003.
[32] a) M. Ciaccia, R. Cacciapaglia, P. Mencarelli, L. Mandolini, S. Di Stefano, *Chem. Sci.* **2013**, *4*, 2253. 10.1039/C3SC50277E; b) M Ciaccia, S. Pilati, R. Cacciapaglia, L. Mandolini, S. Di Stefano, *Org. Biomol. Chem.* **2014**, *12*, 3282–3287. 10.1039/C4OB00107A.
[33] K. A. Palasis, A. D. Abell, *Tetrahedron Letters* **2024**, *138*, 154967. 10.1016/j.tetlet.2024.154967.
[34] R. Göstl, S. Hecht, *Angew. Chem.* **2014**, *126*, 8929–8932; *Angew. Chem. Int. Ed.* **2014**, *53*, 8784–8787. 10.1002/anie.201310626.
[35] A. Fuhrmann, R. Göstl, R. Wendt, J. Kötteritzsch, M. D. Hager, U. S. Schubert, K. Brademann-Jock, A. F. Thünemann, U. Nöchel, M. Behl, S. Hecht, *Nat. Commun.* **2016**, *7*, 13623. 10.1038/ncomms13623.
[36] M. Kathan, P. Kovaříček, C. Jurissek, A. Senf, A. Dallmann, A. F. Thünemann, S. Hecht, *Angew. Chem.* **2016**, *128*, 14086–14090; *Angew. Chem. Int. Ed.* **2016**, *55*, 13882–13886. 10.1002/anie.201605311.
[37] M. Kathan, F. Eisenreich, C. Jurissek, A. Dallmann, J. Gurke, S. Hecht, *Nat. Chem.* **2018**, *10*, 1031–1036. 10.1038/s41557-018-0106-8.
[38] M. Kathan, S. Hecht, *Chem. Soc. Rev.* **2017**, *46*, 5536–5550. 10.1039/C7CS00112F.
[39] A. Goulet-Hanssens, F. Eisenreich, S. Hecht, *Adv. Mater.* **2020**, *32*, 1905966. 10.1002/adma.201905966.

Manuscript received: October 9, 2024
Accepted manuscript online: January 2, 2025
Version of record online: January 16, 2025